Cancer Science
Japanese Cancer Association JCA
Open Access

Protein kinase A inhibition facilitates the antitumor activity of xanthohumol, a valosin-containing protein inhibitor

Yuki Shikata,[1] Tetsuro Yoshimaru,[2] Masato Komatsu,[2] Hiroto Katoh,[3,4] Reiko Sato,[3] Shuhei Kanagaki,[1] Yasumasa Okazaki,[5] Shinya Toyokuni,[5] Etsu Tashiro,[1] Shumpei Ishikawa,[3] Toyomasa Katagiri[2] and Masaya Imoto[1]

[1]Department of Biosciences and Informatics, Faculty of Science and Technology, Keio University, Yokohama; [2]Division of Genome Medicine, Institute for Genome Research, Tokushima University, Tokushima; [3]Department of Genomic Pathology, Medical Research Institute, Tokyo Medical and Dental University, Tokyo; [4]JST, PRESTO, Saitama; [5]Department of Pathology and Biological Responses, Nagoya University Graduate School of Medicine, Nagoya, Aichi, Japan

Key words

Adenylate cyclase, antitumor activity, apoptosis, valosin-containing protein, xanthohumol

Correspondence

Masaya Imoto, Department of Biosciences and Informatics, Faculty of Science and Technology, Keio University, Yokohama, Japan. Tel/Fax: (81) 45-566-1557; E-mail: imoto@bio.keio.ac.jp

Funding Information

JST, PRESTO and JSPS KAKENHI (Grant/Award Number: 15H03116, 16H02481, 221S0001-04, 25710020).

Received October 27, 2016; Revised January 17, 2017; Accepted January 19, 2017

Cancer Sci **108** (2017) 785–794

doi: 10.1111/cas.13175

Xanthohumol (XN), a simple prenylated chalcone, can be isolated from hops and has the potential to be a cancer chemopreventive agent against several human tumor cell lines. We previously identified valosin-containing protein (VCP) as a target of XN; VCP can also play crucial roles in cancer progression and prognosis. Therefore, we investigated the molecular mechanisms governing the contribution of VCP to the antitumor activity of XN. Several human tumor cell lines were treated with XN to investigate which human tumor cell lines are sensitive to XN. Several cell lines exhibited high sensitivity to XN both *in vitro* and *in vivo*. shRNA screening and bioinformatics analysis identified that the inhibition of the adenylate cyclase (AC) pathway synergistically facilitated apoptosis induced by VCP inhibition. These results suggest that there is crosstalk between the AC pathway and VCP function, and targeting both VCP and the AC pathway is a potential chemotherapeutic strategy for a subset of tumor cells.

Xanthohumol (XN) is a prenylated chalcone present in hops (*Humulus lupus* L.) and beer.[1] XN has received much attention in the last two decades, including reports of its various biological properties, such as anti-inflammatory,[2] antioxidant,[3] anti-angiogenic[4] and antibacterial effects.[5] Furthermore, XN harbors anti-tumorigenic effects toward different types of cancer cells[6] via intracellular reactive oxygen species (ROS) induction,[7] NF-κB and Akt inhibition,[4,8] endoplasmic reticulum (ER) stress induction[9] and disruption of the BIG3-PHB2 interaction.[10]

We previously reported that XN binds directly to valosin-containing protein (VCP) and modulates autophagy by inhibiting VCP functions.[11] VCP, also known as p97, belongs to the ATPase associated with diverse cellular activities (AAA) ATPase family and has a wide variety of cellular functions, such as autophagosome maturation,[12,13] endoplasmic reticulum-associated degradation (ERAD)[14] and the enhancement of NF-κB signaling.[15,16] Therefore, our finding that XN modulated the function of VCP may explain how XN exhibited the abovementioned biological effects, such as autophagosome maturation, ER stress induction and NF-κB inhibition. In addition, because clinical studies have identified a correlation among elevated VCP expression and the progression, prognosis and metastatic potential of gastric carcinoma,[17] pancreatic ductal adenocarcinoma[18] and prostate cancer,[19] the antitumor effects of XN can be attributed to the inhibition of VCP function. However, the molecular mechanisms governing the contribution of VCP to the antitumor activity of XN have remained elusive.

In this study, we performed genome-wide shRNA screening and identified the adenylate cyclase (AC) pathway as genes relating to the antitumor activity of XN against human tumor cells. This pathway regulates various cellular functions via activating PKA-dependent phosphorylation.[20] However, there are no reports that show the relevance of AC/PKA pathway inhibition to the antitumor activity of XN targeting VCP.

Material and Methods

Compounds. H-89 was purchased from Cayman Chemical (Ann Arbor, MI, USA). Paclitaxel (PTX) was purchased from Wako Pure Chemical Industries (Osaka, Japan). KT5720 was purchased from Tocris Bioscience (Bristol, UK). Eeyarestatin I (ESI) was purchased from Santa Cruz Biotechnology (Santa Cruz, CA, USA).

Isolation of xanthohumol from hops. Xanthohumol was isolated and purified from Xantho-Flav Pure (Hopsteiner, Germany). The extract was purified by using HPLC (UG 80,

20 mm, 250 mm; Shiseido, Tokyo, Japan) with 70% aqueous MeOH to obtain pure XN as previously described.[11]

Cell lines. Human epidermoid carcinoma A431 cells, human esophageal cancer EC17 cells and human prostate cancer PC-3 cells were provided by M. Kawada (Institute of Microbial Chemistry, Japan). Human esophageal cancer EC109 cells were provided by Columbia University (New York, NY, USA). Human cervical cancer HeLa cells were provided by M. Yoshida (RIKEN, Japan). Human embryonic kidney HEK293T cells were provided by S. Saiki (Juntendo University, Japan). Human colorectal tumor LoVo, HT29, Colo-201, HCT116, LS-174T, SW620, DLD-1, SW48 and SW480 cells, human lung cancer A549 cells, human breast cancer MCF-7 cells, and human melanoma A2058 cells were obtained from the American Type Culture Collection (ATCC, Rockville, MD, USA).

A431 cells were maintained in DMEM supplemented with 5% calf serum (CS), 100 U/mL penicillin G (Sigma-Aldrich, St. Louis, MO, USA), and 0.1 mg/mL kanamycin (Sigma-Aldrich) at 37°C in a humidified atmosphere containing 5% CO_2. EC17, HEK293T, HeLa and MCF-7 cells were maintained in DMEM supplemented with 10% FBS, 100 U/mL penicillin G, and 0.1 mg/mL kanamycin in the same conditions described above. The other cells were maintained in RPMI-1640 medium supplemented with 10% FBS, 100 U/mL penicillin G and 0.1 mg/mL kanamycin, also in the abovementioned conditions.

Cell cycle and apoptosis analysis by flow cytometry. The percentage of cells in different phases of the cell cycle, including the sub-G_1 population, was analyzed by flow cytometry following staining with propidium iodide (PI; Wako Pure Chemical Industries). In brief, cells were seeded in 6-well plates and, following overnight culture, were treated with XN for 48 h. In the co-treatment test for the PKA inhibitor and XN, the cells were pre-treated with PKA inhibitor for 1 h before being treated with XN. Following treatment, cells were harvested and fixed with ice-cold 70% EtOH at 4°C, followed by treatment with 10 μg/mL RNase A (Wako Pure Chemical Industries) for 20 min at 37°C. Subsequently, cells were stained with 50 μg/mL PI. PI fluorescence was measured by EPICS ALTRA (Beckman Coulter, Brea, CA, USA).

To illustrate a waterfall plot, *Z*-score values were calculated using EC_{50} values of each cell viability (X_i), its mean (X_{mean}) and its standard derivation (S) using the following formula:

$$Z - \text{score} = (X_{\text{mean}} - X_i)/S$$

Western blot analysis. Anti-cleaved-PARP, anti-VCP and anti-survivin were purchased from Cell Signaling Technology (Danvers, MA, USA). Anti-β-actin, HRP-linked anti-mouse IgG and HRP-linked anti-rabbit IgG were purchased from Sigma-Aldrich. Cells were immediately harvested and lysed with RIPA buffer (25 mM HEPES, 1.5% TX-100, 1% sodium deoxycholate, 0.1% SDS, 500 mM NaCl, 5 mM EDTA, 50 mM NaF, 0.1 M Na_3VO_4 and cOmplete Protease Inhibitor Cocktail Tablets [Roche, Mannheim, Germany]; pH 7.8). The lysates were centrifuged at 13 000 g for 15 min to remove the insoluble fraction. Equal amounts of total protein were subsequently separated by SDS-polyacrylamide gel electrophoresis before being transferred onto a PVDF membrane (Millipore, Billerica, MA, USA). The membrane was probed with the indicated antibodies. The chemiluminescence signal was detected using an Immobilon Western kit (Millipore) and ChemiDoc XRS+ System (Bio-Rad, Hercules, CA, USA).

Anti-tumor efficacy in the xenograft model. Six-week old female BALB/c nude mice were purchased from Charles River Laboratories (Tokyo, Japan). XN was suspended in DMSO at a concentration of 100 mM, then diluted with PBS to the concentrations indicated and given daily to the mice. Conversely, control mice received a vehicle control of 0.85% DMSO corresponding to 30 mg/kg XN. Each suspension (1×10^7 cells/mouse) of HCT116 and SW480 cells was mixed with an equal volume of Matrigel (BD, Franklin Lakes, NJ, USA) and injected subcutaneously into the left flank of mice. After the tumors developed over a period of 1 week, reaching sizes of approximately 150 mm^3 (calculated as $1/2 \times [\text{width} \times \text{length}^2]$), mice were randomized into four groups of five and administered drugs by intraperitoneal injection for 17 days. Tumor volume was measured with callipers. Thereafter, mice were killed and tumors were dissected; images were captured with a digital camera.

After being killed, the organs (heart, lung, liver, kidney, spleen and pancreas) were removed immediately. A portion of each tissue was fixed in 10% neutral formalin for histological examination, while the remaining tissue sample was frozen, and preserved at −80°C for subsequent immunohistochemistry. All experiments were performed in accordance with the guidelines of the animal facility at Tokushima University.

Immunohistochemical staining of xenografts. Anti-Ki67 antibody [Sp6], (ab16667) was purchased from Abcam (Cambridge, USA).

Anti-rabbit immunoglobulins/HRP antibody (P0448) and Liquid DAB+ (K3468) were purchased from DAKO (Carpinteria, CA, USA). To examine the Ki67 protein expression in HCT116 xenograft tumors, we stained the tissue sections of paraffin-embedded tumors. In brief, 4-μm sections were dewaxed in xylene and ethanol. The slides were subjected to high-temperature antigen retrieval in citric buffer (10 mM, pH 6.0). After antigen retrieval, the slides were dipped in methanol containing H_2O_2 [0.3% (v/v)] for 30 min. After washing with 10 mM PBS at pH 7.4, the slides were incubated with anti-Ki67 (dilution 1:1600) antibody with microwave irradiation. The slides were then washed with PBS three times for 5 min each time; anti-rabbit immunoglobulins/HRP antibody was applied to the slides. After washing with PBS three times, the expression of Ki67 was visualized as brown precipitates with liquid DAB+. After washing with distilled water, nuclear counterstaining was performed with hematoxylin. The nuclear labeling index of the Ki67 staining was determined under microscope (BX-50, Olympus, Tokyo, Japan) for regular pathological diagnosis. In brief, 1000 tumor cells were counted manually and the positive ratio was calculated in each xenograft. Statistical analysis was performed by Graphpad prism 5 (GraphPad Software, La Jolla, CA, USA).[21].

Lentiviral genome-wide shRNA screening. A dose response curve of XN for HCT116 was calculated using xCelligence (ACEA Biosciences, San Diego, CA, USA), an automated cell growth analyzer. HCT116 cells were cultured at a variety of XN concentrations for 48 h and the real-time cell growth rates were recorded by the xCELLigence.

Genome-wide lentiviral shRNA screenings were performed using HCT116 cells. In brief, an shRNA lentivirus library containing approximately 27 500 barcoded shRNA (DECIPHER shRNA Library: Human Module #1, Cellecta, Mountain View, CA, USA) was produced according to the manufacturer's protocol, after which 2.0×10^7 HCT116 cells were infected by the lentivirus and maintained for 48 h after infection. The shRNA lentivirus-infected HCT116 cells were then selected by puromycin (1.0 μg/mL) for 72 h; the selected cells were then separated into two 15-cm culture dishes with an equal number

of cells, one of which contained XN at a 7.0 μM concentration and the other cultured with DMSO as a control. At 72 h after the XN treatment, the HCT116 cells were harvested and their genomic DNA extracted using a QiaAmp DNA Mini Kit (Qiagen, Hilden, Germany). The shRNA-specific barcode regions were then amplified by PCR according to the manufacturer's protocol, with mild modifications for the PCR primers to make the PCR amplicons readable by an Ion PGM System (Thermo Scientific, Waltham, MA, USA). Quantifications of the cellular clone sizes of each shRNA-infected HCT116 population within control or XN-treated culture conditions were calculated based on the sequence read counts within each sample. shRNA that suppress growth of infected cells in synergy with XN should show significant decreases in the sequence read counts specifically under the XN condition. Therefore, genes that exhibited more than fivefold high frequencies in DMSO-treated cells compared to the XN-treated cells were selected as "hit genes." Thereafter, Gene Ontology-based bioinformatics analysis was performed for the hit genes using the DAVID bioinformatics database focusing on molecular functions and biological processes.[22,23].

Growth inhibition assay and isobologram test. Cell growth was measured by using an MTT assay. In brief, cells were seeded in 96-well plates and, after overnight culture, were treated with H-89 or KT5720 for 1 h. Thereafter, cells were treated with XN, ESI or PTX for an additional 72 h. Following treatment, cells were treated with 0.5 mg/mL MTT (Sigma-Aldrich) for 4 h at 37°C, and lysed with DMSO. Absorbance at 595 nm was measured by a Multiskan FC (Thermo Scientific) and IC_{50} values of each combination of two agents were calculated and plotted on the graph.

For each combination experiment, the combination indexes (CI) were calculated and normalized with IC_{50} values as reported[24] and plotted on an isobologram graph.[25] On the isobologram, a straight line connecting the x-intercepts and y-intercepts and the intervening points infers an additive effect between two agents. Conversely, a concave or convex line infers a synergism or an antagonism between the two agents, respectively.

Results

Xanthohumol exhibited antitumor activity *in vitro* and *in vivo*. First, we examined the effect of XN on 18 different human tumor cell lines chosen in a random manner. Each cell was treated with XN for 48 h and the sub-G_1 populations were determined via flow cytometry. *Z*-score values were then calculated using EC_{50} values of cell viability and plotted on a waterfall plot. As shown in Figure 1(a), seven cell lines, including SW480, SW48, DLD-1, SW620, A2058, LS-174T and HCT116 cells, were highly sensitive to XN. However, there were not significant differences in VCP expression levels between XN-sensitive cells and the other cell lines (Fig. 1b). Subsequently, we detected the expression levels of cleaved-PARP by western blot to confirm the apoptosis-inducing ability of XN. As shown in Figure 1(c), when XN-sensitive SW480 and HCT116 cells and XN-insensitive HT29 and A549 cells were treated with indicated concentrations of XN for 24 h, the expression levels of cleaved-PARP increased in XN-sensitive SW480 and HCT116 cells, but not in HT29 and A549 cells. We correlated these results with a waterfall plot analysis.

We next investigated the antitumor effects of XN against XN-sensitive cells *in vivo*. Human colorectal tumor HCT116 and SW480 cells were injected subcutaneously into nude mice to establish xenograft models. Mice were randomized into four groups of five, after which the vehicle or XN was administered by intraperitoneal injection. As shown in Figure 1(d,e), tumor growth inhibition was observed in each xenograft model in a dose-dependent manner, without significant body weight loss (Fig. 1f). Furthermore, we evaluated its effect on Ki67 labeling index as a tumor proliferative index using immunohistochemical (IHC) methods. A significant reduction of Ki67 labeling index in tumors was observed in dose-dependent manner (Fig. 1g). These results indicated that XN exhibited antitumor activity against several human tumor cell lines *in vitro* and *in vivo*.

shRNA screening reveals the adenylate cyclase pathway is correlated with xanthohumol-induced cell death. To identify the key genes playing a critical role in XN-induced cell death, we generated a lentiviral-based shRNA screening system and screened for genes related to the antitumor activity of XN using HCT116 cells. Before the screening, we determined the drug concentration to be somewhat lower than the IC_{50} value because at the concentration of IC_{50}, the shRNA-infected cells exhibit too many "random deaths" due only to the drug function without the synthetic shRNA effects. In our study, to decide on the concentration of XN for the shRNA screening, we performed a growth inhibition assay and the IC_{50} value was calculated. A dose response curve of XN for HCT116 is shown in Figure S1, and the IC_{50} value was approximately 8.1 μM. Then, we decided to conduct the shRNA screening at the concentration of 7.0 μM XN, at a lower concentration compared to the IC_{50}, based on the abovementioned theoretical background.

Next, HCT116 cells were infected with a mixture of approximately 27 500 barcoded shRNA and cultured in the presence of either 7.0 μM XN or DMSO. After 3 days, genomic DNA was isolated from the cells and the shRNA-specific barcode regions were amplified by PCR with the lentivirus vector-specific primers. The abundance of each shRNA was then quantified by high-throughput sequencing (Fig. 2). As a result, 138 shRNA, which exhibited more than fivefold high frequencies in DMSO-treated cells compared to XN treated cells, were selected as the hit genes (Table S1). This suggests that knockdown of these genes enhances the antitumor activity of XN, because HCT116 cells infected with these 138 shRNA showed growth inhibition specifically under the synergic XN culture condition. Subsequently, Gene Ontology-based bioinformatics analysis was performed on the hits using the DAVID bioinformatics database.[22,23] As a result, Gene Ontology-term enrichment analysis of the hit genes, focusing on molecular functions and biological processes, showed strong enrichment of genes involved in adenylate cyclase activity (Tables S2 and S3). These results raised the possibility that the adenylate cyclase pathway may play a crucial role in XN-induced cell death.

Protein kinase A inhibitors enhanced the antitumor activity of valosin-containing protein inhibitors. The Adenylate cyclase (AC) pathway, also known as the cyclic AMP (cAMP)-dependent pathway, is a well-known G protein-coupled receptor-regulated signaling cascade. The G protein families, including G_i and G_s, regulate AC activity. AC catalyzes the conversion of ATP to cAMP, which, in turn, regulates cellular function via activating protein kinase A (PKA)-dependent phosphorylation.[20] Therefore, to examine whether the suppression of the AC/PKA pathway could synergistically enhance the antitumor activity of XN, we performed an MTT assay using the PKA inhibitor H-89[26] and graphically plotted the results on isobolograms.[24,25] HCT116 cells were treated with various concentrations of XN in the presence or absence of H-89 for

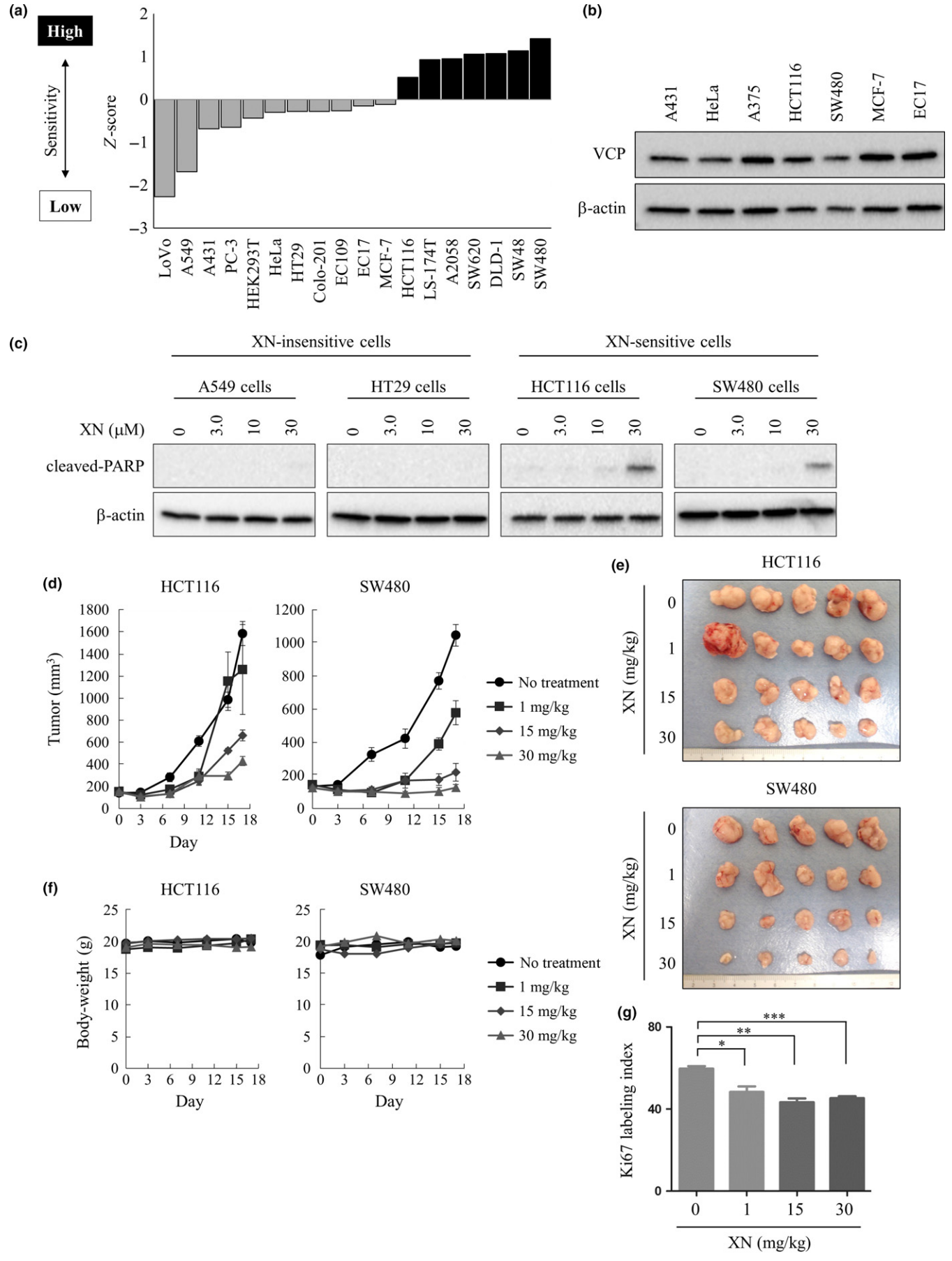

Fig. 1. Antitumor activities of xanthohumol *in vitro* and *in vivo*. The effects of xanthohumol (XN) on several types of human tumor cell lines and xenograft models were examined. (a) The sub-G_1 populations were determined 48 h after XN treatment via flow cytometry. *Z*-score values were calculated as described in the Materials and Methods and plotted on a waterfall plot. (b) The expression levels of valosin-containing protein (VCP) in several human tumor cells were detected by western blot. (c) XN-sensitive SW480 and HCT116 cells and XN-insensitive HT29 and A549 cells were treated with XN for 24 h and the expression levels of cleaved-PARP were detected by western blot. (d–f) Human colorectal tumor HCT116 and SW480 cells, the XN-sensitive cells, were injected subcutaneously into nude mice to establish xenograft models. After the tumors developed over a period of 1 week, reaching sizes of approximately 150 mm^3, mice were randomized into four groups of five, after which the vehicle or XN was administered daily by intraperitoneal injection for 17 days. Tumor size and body weight were measured and tumors were dissected and imaged with a digital camera. (g) Dose-dependent inhibition of Ki67 labeling index by XN treatment in tumor xenografts *in vivo*. Nuclear Ki67 labeling index at indicated dose levels was determined in HCT116 tumors on study day 17.

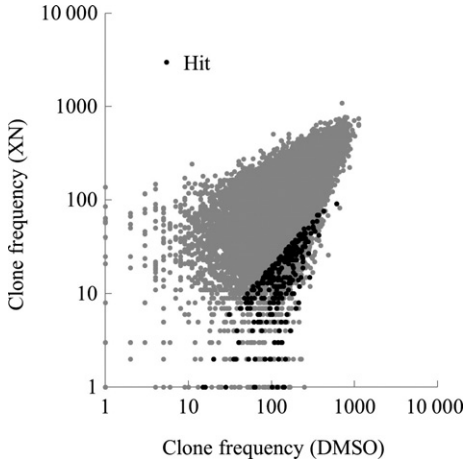

Fig. 2. shRNA screening for the identifications of key factors modulating antitumor activity of xanthohumol. A lentiviral-based shRNA screening was performed for screening genes related to the antitumor activity of xanthohumol (XN). HCT116 cells were infected with an shRNA lentivirus library containing approximately 27 500 shRNA and then cultured in the presence or absence of 7.0 μM XN for 3 days. Genomic DNA was isolated and amplified by PCR targeting shRNA-specific barcode regions. Each shRNA was then quantified by high-throughput sequencing. The *x*-axis and *y*-axis represent clone frequency of each shRNA from the cells cultured with DMSO and XN, respectively. The hit genes that exhibited more than fivefold high frequencies in DMSO-treated cells compared to the XN-treated cells are represented by black dots.

72 h and cell viability was measured by MTT assay. IC_{50} values of each combination of two agents and the combination indexes (CI) were then calculated and plotted on an isobologram. The combination of H-89 with XN produced a concave line, indicating a synergistic interaction (Fig. 3a). Similar results were obtained when another PKA inhibitor, KT5720,[27] was used instead of H-89 (Fig. 3b). Conversely, when using the non-specific cytotoxic agent paclitaxel (PTX) instead of XN, H-89 plus PTX produced a straight line, indicating an additive interaction in the HCT116 cells (Fig. 3c). Thus, PKA inhibition is responsible for synergistically enhancing the antitumor activity of XN. We then performed similar tests using another VCP inhibitor, eeyarestatin I (ESI).[28] As shown in Figure 3(d), the combinations of H-89 with ESI produced a concave line, indicating a synergistic interaction in HCT116 cells. Furthermore, the synergistic effect of H-89 and XN was confirmed in the other human tumor cell lines, XN-sensitive SW480 and XN-insensitive HT29 cells (Fig. 3e,f). These results suggest that the inhibition of AC/PKA pathway synergistically enhances the antitumor activity of VCP inhibitors, including XN and ESI, in various types of human tumor cell lines.

Synergistic effect of protein kinase A inhibition and xanthohumol on apoptosis induction. We next investigated whether the combination of PKA inhibitors with XN exhibited a synergistic interaction on apoptosis induction. HCT116 cells were treated with the indicated concentrations of XN in the presence or absence of 10 μM H-89 or KT5720 for 48 h, after which sub-G_1 populations were measured by PI-stain and flow cytometry. As shown in Figure 4(a,b), co-treatment of PKA inhibitors and XN synergistically increased sub-G_1 populations compared to XN alone, indicating that PKA inhibitors affected the apoptosis-inducing activity of XN. Interestingly, XN or H-89 alone did not increase the sub-G_1 population in HT29, A549 and LoVo cells. However, combinations with H-89 could increase the sub-G_1 population in these cell lines, indicating that H-89 treatment might facilitate XN-induced apoptosis also in XN-insensitive cells (Fig. 4c–e).

Discussion

Xanthohumol, a simple prenylated chalcone, is the most well studied compound isolated from hops because of its potential as a cancer chemopreventive agent against several human tumor cell lines.[29–31] Therefore, many researchers have proposed various molecular mechanisms explaining how XN exhibits antitumor activity. However, until now, there have been no reports of the contribution of valosin-containing protein (VCP) inhibition to XN's antitumor activity. VCP may play crucial roles in cancer progression, prognosis and recurrence,[17–19] and we previously reported that XN directly binds to VCP and inhibits its functions.[11] Therefore, in the current work, we examined the antitumor activity of XN targeting VCP.

We first investigated which human tumor cell lines were sensitive to XN, revealing several cell lines highly sensitive to XN *in vitro*. Overexpression of VCP occurs in many cancers and clinical studies have reported a correlation between elevated VCP expression and its progression.[32] However, because significant differences in the expression levels of VCP were not found among the cell lines we tested, XN sensitivity is not dependent on VCP expression levels. Conversely, another VCP inhibitor, eeyarestatin I (ESI), showed antitumor effects in tumor cells with a similar waterfall profile to XN (Fig. S2), indicating that inhibition of VCP function is responsible for cell viability in XN-sensitive tumor cells. VCP functions as a critical mediator of protein homeostasis. VCP is essential to some aspects of ubiquitin-dependent proteasomal degradation, including endoplasmic reticulum-associated degradation (ERAD), which degrades misfolded proteins. VCP is also involved in the aggresome–autophagy pathway, which is required for clearing misfolded proteins that form aggregates in the cytosol. The malignant transformation may result in cell deregulation often associated with cellular stress, such as accumulation of misfolded proteins; adaptation to this stress phenotype is required for tumor cells to survive. Therefore, although the detailed function of VCP in XN-sensitive tumor cells remains unclear, subsets of tumor cells (XN-sensitive tumor cells) may, in turn, depend on VCP function.

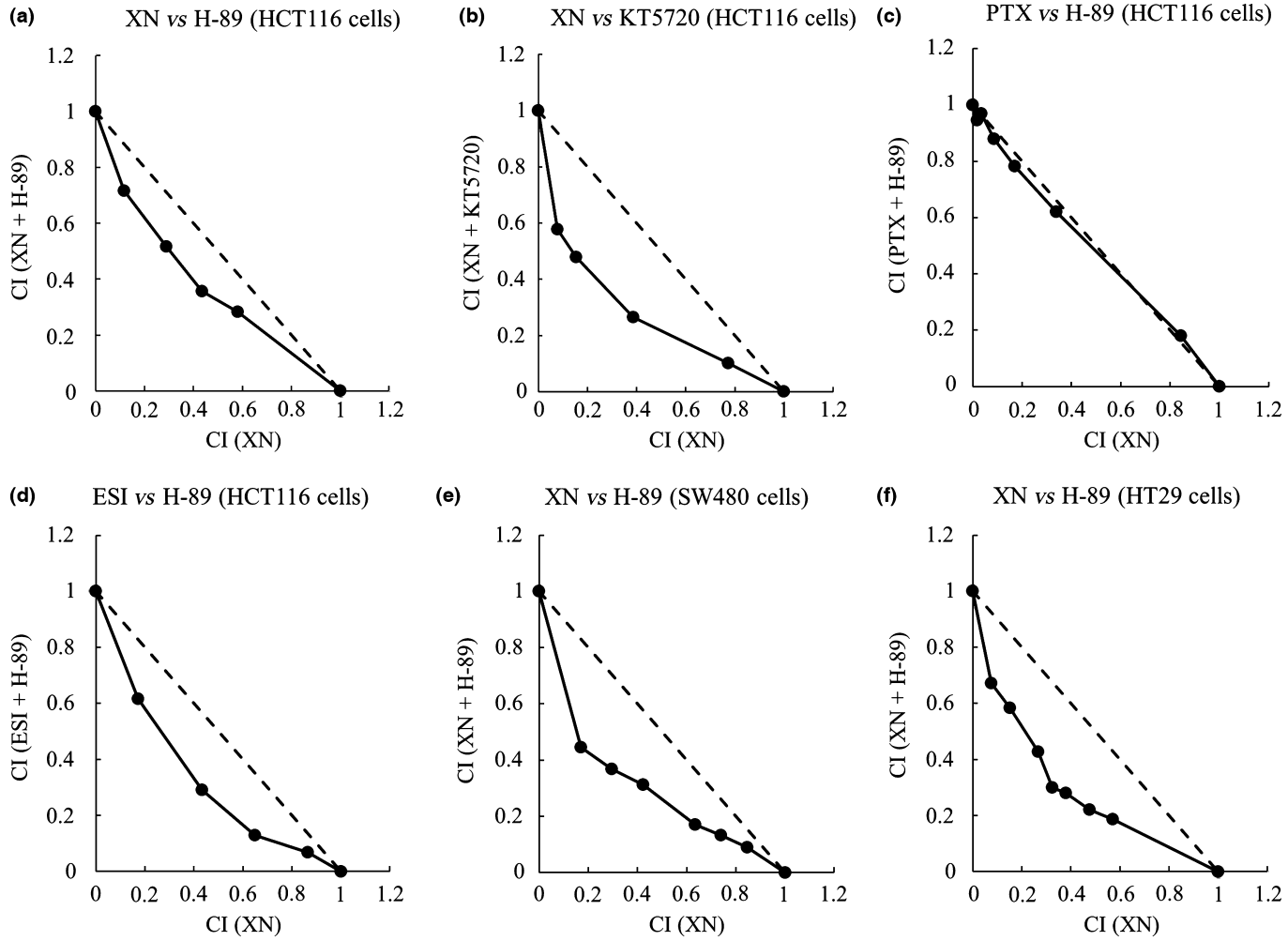

Fig. 3. Combination experiment of protein kinase A and valosin-containing protein inhibition. To investigate the combination efficacy between protein kinase A (PKA) and valosin-containing protein (VCP) inhibition, an MTT assay was performed and the isobologram was plotted. (a,b) HCT116 cells were treated with various concentrations of xanthohumol (XN) in the presence or absence of H-89 or KT5720 for 72 h and the cell viability was measured by MTT assay. The combination index (CI) for each combination of two agents was calculated using the IC_{50} value and plotted on the isobologram, as described in the Materials and Methods. (c) Paclitaxel, a non-specific cytotoxic agent as a negative control, was used instead of XN in HCT116 cells. As described above, CI was calculated and the isobologram was plotted. (d) Eeyarestatin I, another VCP inhibitor, was used instead of XN in HCT116 cells. As described above, CI was calculated and the isobologram was plotted. (e,f) The synergistic effect of H-89 and XN was confirmed in the other human tumor cell lines, XN-sensitive SW480 and XN-insensitive HT29 cells. Each cell was treated with various concentrations of XN in the presence or absence of H-89 for 72 h and the isobologram was plotted.

Previously, Yoshimaru *et al.* report that XN treatment (0.3–1.0 mg/kg) significantly inhibited estrogen (E2)-induced tumor growth through specific disruption of the BIG3–PHB2 interaction, regardless of VCP function *in vivo*.[10] Conversely, the lower dose range of XN did not show significant antitumor effects on the human colorectal tumor HCT116 and SW480 cells *in vivo*, but significant tumor growth inhibition was observed in these cells in response to daily intraperitoneal injection of higher doses of XN (15–30 mg/kg), possibly through VCP inhibition. Notably, no morphological changes were observed in the heart, lung, liver, kidney, spleen and pancreas of mice, despite receiving high doses of XN (30 mg/kg) daily for 17 days (Fig. S3). However, what determines the sensitivity to XN remained elusive. When we compared the effect of XN on the expression levels of several pro-apoptosis and anti-apoptosis proteins in XN-sensitive cells, only expression levels of survivin were found to be affected by XN. XN induced a decrease in the expression levels of survivin in XN-sensitive cells (HCT116 and SW480 cells) in a dose-dependent manner; however, XN weakly suppressed the expression levels of survivin in XN-insensitive tumor cells (A549 and HT29 cells), as shown in Figure S4. Therefore, it is likely that the effect of XN on survivin expression may be related to the sensitivity of tumor cells to XN.

We also determined which key factors modulate the apoptosis-inducing activity of XN. For this, we performed shRNA screening and bioinformatics analysis. Interestingly, the adenylate cyclase (AC) pathway-related genes were hits, indicating that the AC pathway plays a crucial role in XN-inducing apoptosis. The AC pathway is known to activate protein kinase A (PKA) phosphorylation via converting ATP to cyclic AMP (cAMP) and regulating target genes.[20] We found in this study that in the tumor cell lines we tested, the inhibition of PKA, a downstream kinase of AC and cAMP, enhanced the apoptosis-inducing activity of XN. These results raised the possibility that the AC/PKA pathway could contribute to preventing apoptosis induced by VCP inhibition and that the activity of AC/PKA pathway in tumor cells could determine sensitivity to XN.

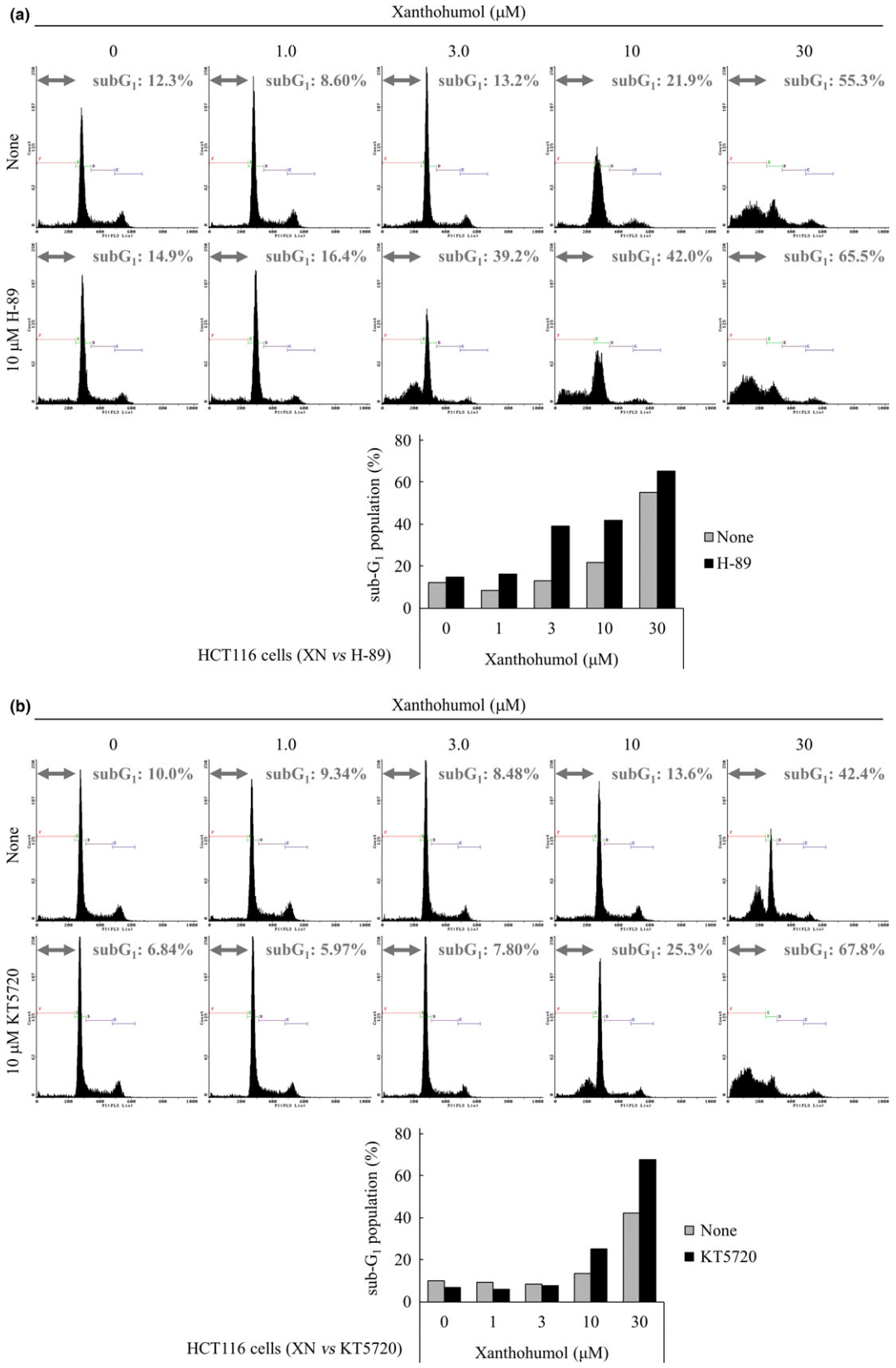

Fig. 4. The combination efficacy of protein kinase A inhibition and xanthohumol on apoptosis induction. The sub-G_1 population was measured via flow cytometry to investigate whether the combination of protein kinase A (PKA) inhibitor with xanthohumol (XN) exhibits the synergistic interaction on apoptosis induction. (a,b) HCT116 cells were treated with various concentrations of XN in the presence or absence of H-89 or KT5720 for 48 h and the sub-G_1 populations were measured via flow cytometry. (c–e) The synergistic effect of H-89 and XN was confirmed in the other human tumor cell lines, XN-insensitive HT29, A549 and LoVo cells. Cells were treated with various concentrations of XN in the presence or absence of H-89 for 48 h and the sub-G_1 populations were measured as described above.

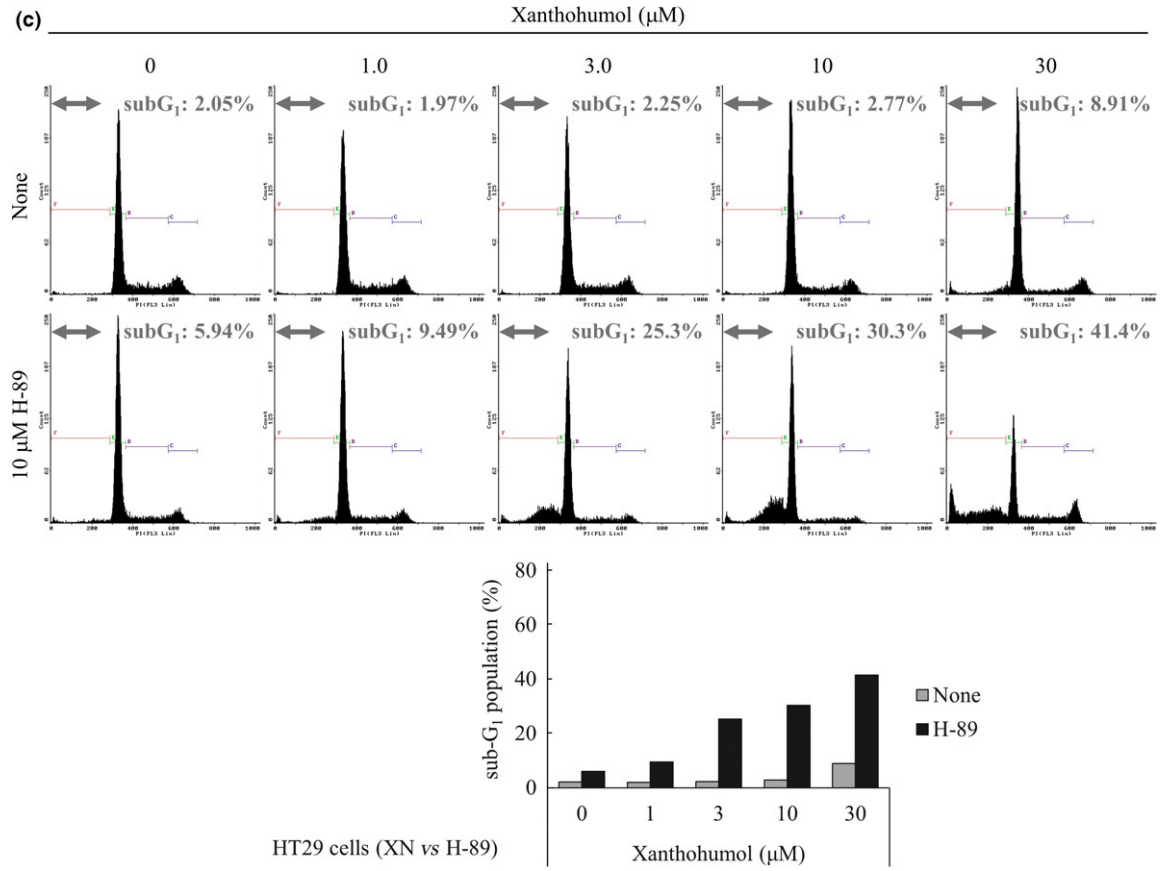

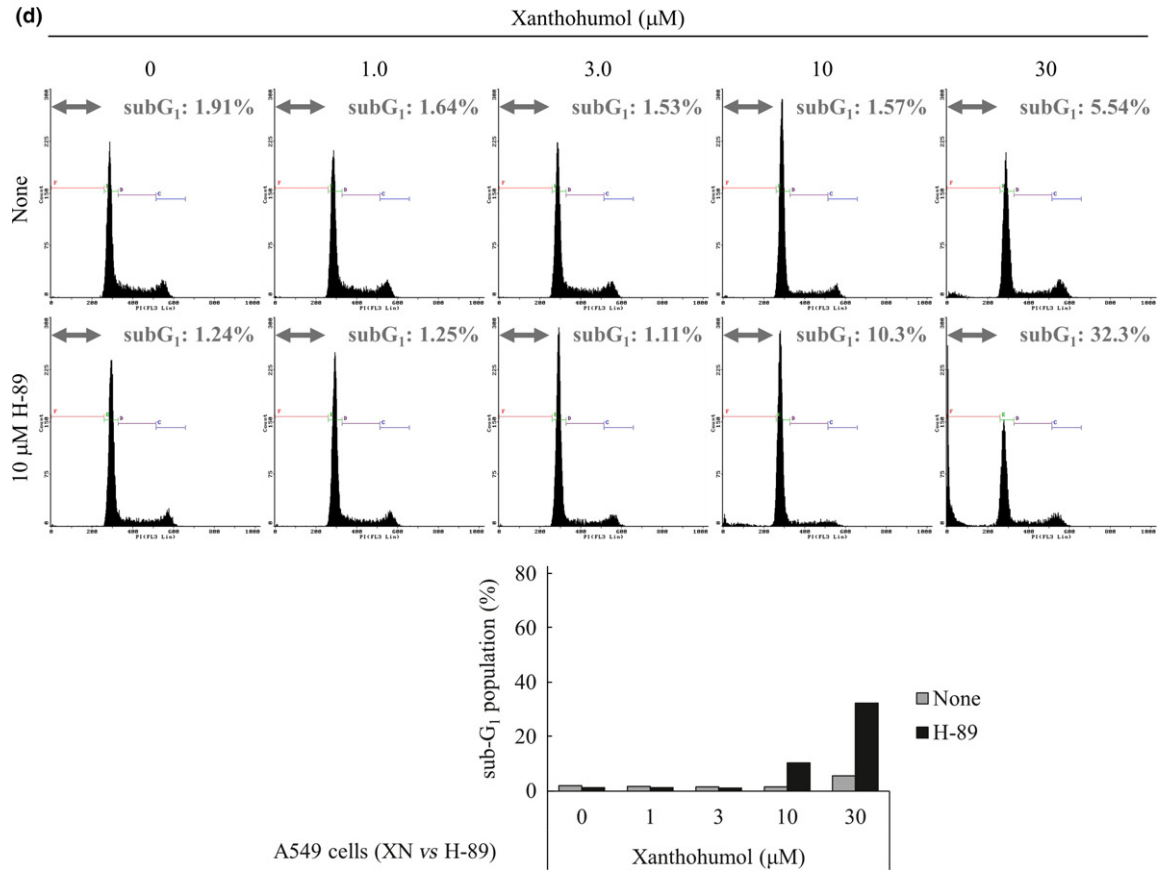

Fig. 4. continued.

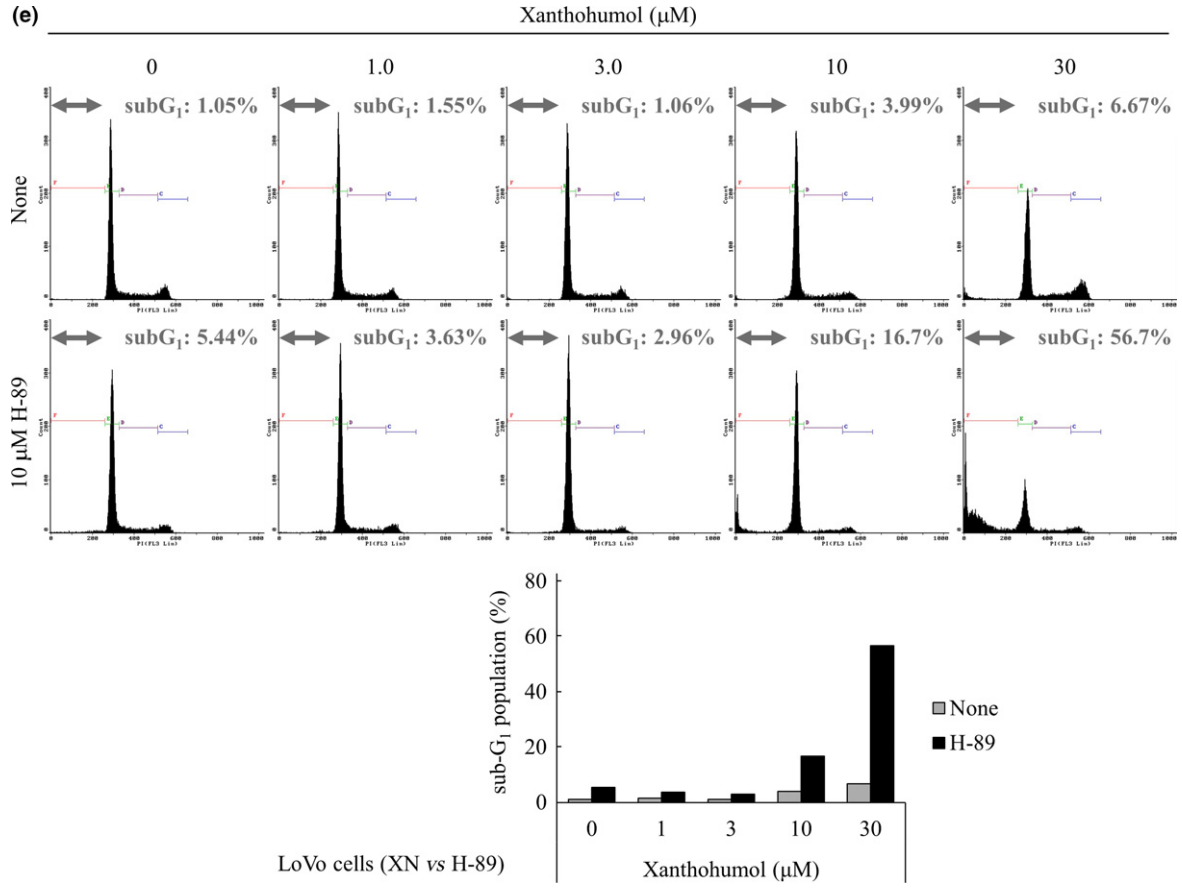

Fig. 4. continued.

Recently, it has been reported that XN acts at GABAA receptors present in the hippocampal nerve terminals to decrease the Ca^{2+} influx through N-type and P/Q-type Ca^{2+} channels, which subsequently suppresses the Ca^{2+}-calmodulin/PKA cascade to decrease the evoked glutamate release.[33] These results indicated that XN-mediated decrease in the Ca^{2+} influx caused the suppression of the PKA cascade in the rat hippocampus, and, therefore, H-89 has been shown to largely prevent the inhibition of glutamate release by XN. In contrast, we found that H-89 did not prevent apoptosis by XN; rather, it synergistically enhanced the antitumor activity of XN. Therefore, XN did not induce the suppression of PKA in tumor cells, and the target of XN to induce apoptosis was different from that of PKA inhibitors.

The next question was how the AC/PKA pathway prevented apoptosis signals induced by VCP inhibition. Several previous studies have reported the anti-apoptotic role of AC/PKA in various types of cells; however, the mechanisms through which PKA works are often not known. One well-described anti-apoptotic role of PKA is that PKA inhibition induces a decrease in expression levels of survivin, an anti-apoptotic protein, in human colorectal tumor SW480 cells.[34] We also found that H-89 at 10 μM suppressed the expression levels of survivin in XN-sensitive and XN-insensitive tumor cells. In addition, suppressed expression of survivin by H-89 was further enhanced in the presence of XN (Fig. S4). Therefore, decreased expression of survivin by both PKA inhibition and VCP inhibition may be responsible for the synergistic enhancement of apoptosis by VCP inhibition and PKA inhibition. Further studies will be necessary to exactly delineate the factors contributing to the suppression of survivin expression by XN or PKA inhibitor.

In conclusion, our findings suggest that several human tumor cell lines require VCP function for their survival, and that targeting both VCP and the AC/PKA pathway is a potential chemotherapeutic strategy for the subset of tumor cells.

Acknowledgments

This work was supported by JSPS KAKENHI Grant Number 15H03116 for M.I., JSPS KAKENHI Grant Numbers 16H02481 and 25710020 for S.I., and JSPS KAKENHI Grant Number 221S0001-04 for S.T.; this research was also supported by JST, PRESTO for H.K.

Disclosure Statement

The authors have no conflict of interest to declare.

References

1 Power FB, Tutin F, Rogerson H. CXXXV.—The constituents of hops. *J Chem Soc Trans* 1913; **103**: 1267–92.

2 Cho Y-C, Kim HJ, Kim Y-J, *et al.* Differential anti-inflammatory pathway by xanthohumol in IFN-γ and LPS-activated macrophages. *Int Immunopharmacol* 2008; **8**: 567–73.

3 Vogel S, Ohmayer S, Brunner G, Heilmann J. Natural and non-natural prenylated chalcones: synthesis, cytotoxicity and anti-oxidative activity. *Bioorg Med Chem* 2008; **16**: 4286–93.
4 Albini A, Dell'Eva R, Vené R, *et al.* Mechanisms of the antiangiogenic activity by the hop flavonoid xanthohumol: NF-κB and Akt as targets. *FASEB J* 2006; **20**: 527–9.
5 Bhattacharya S, Virani S, Zavro M, Haas GJ. Inhibition of streptococcus mutans and other oral streptococci by hop (*Humulus lupulus* L.) constituents. *Econ Bot* 2003; **57**: 118–25.
6 Dorn C, Bataille F, Gaebele E, Heilmann J, Hellerbrand C. Xanthohumol feeding does not impair organ function and homoeostasis in mice. *Food Chem Toxicol* 2010; **48**: 1890–7.
7 Festa M, Capasso A, D'Acunto CW, *et al.* Xanthohumol induces apoptosis in human malignant glioblastoma cells by increasing reactive oxygen species and activating MAPK pathways. *J Nat Prod* 2011; **74**: 2505–13.
8 Deeb D, Gao X, Jiang H, Arbab AS, Dulchavsky S, Gautam SC. Growth inhibitory and apoptosis-inducing effects of xanthohumol, a prenylated chalone present in hops, in human prostate cancer cells. *Anticancer Res* 2010; **30**: 3333–9.
9 Lust S, Vanhoecke B, Van Gele M, *et al.* Xanthohumol activates the proapoptotic arm of the unfolded protein response in chronic lymphocytic leukemia. *Anticancer Res* 2009; **29**: 3797–805.
10 Yoshimaru T, Komatsu M, Tashiro E, *et al.* Xanthohumol suppresses oestrogen-signalling in breast cancer through the inhibition of BIG3-PHB2 interactions. *Sci Rep* 2014; **4**: 7355.
11 Sasazawa Y, Kanagaki S, Tashiro E, *et al.* Xanthohumol impairs autophagosome maturation through direct inhibition of valosin-containing protein. *ACS Chem Biol* 2012; **7**: 892–900.
12 Ju J-S, Fuentealba RA, Miller SE, *et al.* Valosin-containing protein (VCP) is required for autophagy and is disrupted in VCP disease. *J Cell Biol* 2009; **187**: 875–88.
13 Tresse E, Salomons FA, Vesa J, *et al.* VCP/p97 is essential for maturation of ubiquitin-containing autophagosomes and this function is impaired by mutations that cause IBMPFD. *Autophagy* 2010; **6**: 217–27.
14 Yamanaka K, Sasagawa Y, Ogura T. Recent advances in p97/VCP/Cdc48 cellular functions. *Biochim Biophys Acta* 2012; **1823**: 130–7.
15 Dai R-M, Chen E, Longo DL, Gorbea CM. Li C-CH. involvement of valosin-containing protein, an ATPase Co-purified with IκBα and 26 S proteasome, in ubiquitin-proteasome-mediated degradation of IκBα. *J Biol Chem* 1998; **273**: 3562–73.
16 Asai T, Tomita Y, Nakatsuka S, *et al.* VCP (p97) regulates NFkB signaling pathway, which is important for metastasis of osteosarcoma cell line. *Jpn J Cancer Res* 2002; **93**: 296–304.
17 Yamamoto S, Tomita Y, Hoshida Y, *et al.* Expression level of valosin-containing protein is strongly associated with progression and prognosis of gastric carcinoma. *J Clin Oncol* 2003; **21**: 2537–44.
18 Yamamoto S, Tomita Y, Hoshida Y, *et al.* Increased expression of valosin-containing protein (p97) is associated with lymph node metastasis and prognosis of pancreatic ductal adenocarcinoma. *Ann Surg Oncol* 2004a; **11**: 165–72.
19 Tsujimoto Y, Tomita Y, Hoshida Y, *et al.* Elevated expression of valosin-containing protein (p97) is associated with poor prognosis of prostate cancer. *Clin Cancer Res* 2004; **10**: 3007–12.
20 Ostrom RS, Post SR, Insel PA. Stoichiometry and compartmentation in G protein-coupled receptor signaling: Implications for therapeutic interventions involving Gs. *J Pharmacol Exp Ther* 2000; **294**: 407–12.
21 Okazaki Y, Nagai H, Chew SH, *et al.* CD146 and insulin-like growth factor 2 mRNA-binding protein 3 predict prognosis of asbestos-induced rat mesothelioma. *Cancer Sci* 2013; **104**: 989–95.
22 Huang DW, Sherman BT, Lempicki RA. Systematic and integrative analysis of large gene lists using DAVID bioinformatics resources. *Nat Protoc* 2009a; **4**: 44–57.
23 Huang DW, Sherman BT, Lempicki RA. Bioinformatics enrichment tools: Paths toward the comprehensive functional analysis of large gene lists. *Nucleic Acids Res* 2009b; **37**: 1–13.
24 Chou T-C. Theoretical basis, experimental design, and computerized simulation of synergism and antagonism in drug combination studies. *Pharmacol Rev* 2006; **58**: 621–81.
25 Hall M, Middleton R, Westmacott D. The fractional inhibitory concentration (FIC) index as a measure of synergy. *J Antimicrob Chemother* 1983; **11**: 427–33.
26 Chijiwa T, Mishima A, Hagiwara M, *et al.* Inhibition of forskolin-induced neurite outgrowth and protein phosphorylation by a newly synthesized selective inhibitor of cyclic AMP-dependent protein kinase, N-[2-(p-bromocinnamylamino) ethyl]-5-isoquinolinesulfonamide (H-89), of PC12D pheochromocytoma cells. *J Biol Chem* 1990; **265**: 5267–72.
27 Kase H, Iwahashi K, Nakanishi S, *et al.* K-252 compounds, novel and potent inhibitors of protein kinase C and cyclic nucleotide-dependent protein kinases. *Biochem Biophys Res Commun* 1987; **142**: 436–40.
28 Wang Q, Li L, Ye Y. Inhibition of p97-dependent protein degradation by Eeyarestatin I. *J Biol Chem* 2008a; **283**: 7445–54.
29 Gerhauser C, Alt A, Heiss E, *et al.* Cancer chemopreventive activity of xanthohumol, a natural product derived from hop. *Mol Cancer Ther* 2002; **1**: 959–69.
30 Vanhoecke B, Derycke L, Van Marck V, Depypere H, De Keukeleire D, Bracke M. Antiinvasive effect of xanthohumol, a prenylated chalcone present in hops (*Humulus lupulus* L.) and beer. *Int J Cancer* 2005; **117**: 889–95.
31 Stevens JF, Page JE. Xanthohumol and related prenylflavonoids from hops and beer: to your good health!. *Phytochemistry* 2004; **65**: 1317–30.
32 Yamamoto S, Tomita Y, Hoshida Y, *et al.* Expression of valosin-containing protein in colorectal carcinomas as a predictor for disease recurrence and prognosis. *Clin Cancer Res* 2004b; **10**: 651–7.
33 Chang Y, Lin TY, Lu CW, Huang SK, Wang YC, Wang SJ. Xanthohumol-induced presynaptic reduction of glutamate release in the rat hippocampus. *Food Funct* 2016; **7**: 212–26.
34 Wang D, Wang H, Ning W, Backlund MG, Dey SK, DuBois RN. Loss of cannabinoid receptor 1 accelerates intestinal tumor growth. *Cancer Res* 2008b; **68**: 6468–76.

Supporting Information

Additional Supporting Information may be found online in the supporting information tab for this article:

Fig. S1. A dose response curve of xanthohumol (XN) on HCT116 cells for a global shRNA screening.

Fig. S2. Antitumor activities of eeyarestatin I *in vitro* and a waterfall plot.

Fig. S3. Representative morphological observations of dissected heart, lung, liver, kidney, spleen, and pancreas from mice.

Fig. S4. Involvement of survivin in xanthohumol-induced apoptosis.

Table S1. Hit genes identified by shRNA screening.

Table S2. Gene Ontology based bioinformatics analysis using DAVID bioinformatics database, focusing on molecular functions.

Table S3. Gene Ontology based bioinformatics analysis using DAVID bioinformatics database, focusing on biological processes.